Synthesis, Structure and Magnetism of Homologous Series of Polycrystalline Cobalt Alkane Mono- and Dicarboxylate Soaps

Jean-Michel Rueff,[a] Norberto Masciocchi,*[b, c] Pierre Rabu,*[a] Angelo Sironi,[b] and Antoine Skoulios[a]

Abstract: Carboxylate-bridged chain complexes of Co^{II} (the diaquacobalt(II) mono- and α,ω-dialkanoates) form two homologous series of layered compounds which have been fully characterised both structurally and magnetically. The crystal structures of two selected members, $[Co\{CH_3(CH_2)_{10}COO\}_2(H_2O)_2]$ and $[Co\{CH_3(CH_2)_{18}COO\}_2(H_2O)_2]$, have been solved by X-ray powder diffraction and selected-area electron diffraction methods, and refined by the Rietveld technique. Crystal data: monoclinic, $P2_1/a$; $a = 9.688(1)$, $b = 7.5495(9)$, $c = 37.281(5)$ Å, $\beta = 96.70(3)^\circ$, $Z = 4$; and monoclinic, $P2_1/a$; $a = 9.7260(7)$, $b = 7.5477(7)$, $c = 57.53(1)$ Å, $\beta = 94.66(4)^\circ$, $Z = 4$, respectively. Their isomorphous structures contain layers of octahedral diaquacobalt(II) ions bonded to two chemically inequivalent alkanoates, one chelating and one bridging two Co atoms about 6.3 Å apart, thus confirming the rare *anti–anti* conformation mode of the μ-RCOO groups recently proposed for diaquacobalt(II) α,ω-dodecanedioate. Extensive magnetic characterisation allowed estimation of the feeble antiferromagnetic coupling, which is weaker in the mono- than in the dialkanoate series.

Keywords: carboxylate ligands · cobalt · layered compounds · magnetic properties · X-ray diffraction

Introduction

In a recent paper[1] devoted to a methodical investigation of low-dimensional magnetic compounds in which the magnetic centres are arranged in well-separated two-dimensional layers, the case of diaquacobalt(II)-*n*-dodecane-α,ω-dioate was reported. Its crystal structure was established by the joint use of X-ray powder diffraction (XRPD) and selected-area electron diffraction (SAED) experiments. We showed that it contains stacked layers of bis-aquated cobalt(II) ions connected by carboxylato bridges, of both chelating and bridging type, forming [Co-OCO-Co] chains throughout the crystals. These layers are separated by alkyl chains arranged nearly perpendicularly to the polar sheets. The magnetic properties were then investigated and the weak antiferromagnetism observed ($J = -2.08$ K) was attributed to the rare *anti–anti* conformation of the Co-OCO-Co fragments in the Co^{II} chains.

Following this preliminary report, the present paper is intended, firstly, to outline the synthesis of two homologous series of long-chained cobalt(II) soaps $[Co^{II}\{OOC(CH_2)_{n-2}COO\}(H_2O)_2]$ and $[Co^{II}\{CH_3(CH_2)_{n-2}COO\}_2(H_2O)_2]$ (i.e., diaquacobalt(II) *n*-alkane-α,ω-dioate, ***d-n* Co**, and diaquacobalt(II) *n*-alkanoate, ***m-n* Co**), then to describe their detailed crystal structures as determined by combining ab initio XRPD techniques (very recently reviewed in ref. [2]) with electron diffraction, and finally to discuss their magnetic behaviour in terms of chemical bonding and crystal structure. Moreover, the results presented hereafter may be of broader significance, leading to a structural interpretation of the properties of transition metal soaps, which have been extensively used in the past as lubricants, corrosion inhibitors, catalysts, polymer stabilisers, germicides and in the paint, varnish and color printing industry.[3]

Results and Discussion

Synthesis: Compounds ***m-n* Co**, with *n* even and ranging from 12 to 22, and compounds ***d-n* Co**, with *n* even and ranging from 8 to 16, were prepared in two steps by metathesis in water/

[a] Dr. P. Rabu, Dr. J.-M. Rueff, Dr. A. Skoulios
Institut de Physique et Chimie des Matériaux de Strasbourg
UMR 7504 CNRS-ULP-ECPM
23 rue du Loess, 67037 Strasbourg Cedex (France)
Fax: (+33) 3 88 10 72 47
E-mail: pierre.rabu@ipcms.u-strasbg.fr

[b] Prof. N. Masciocchi, Prof. A. Sironi
Dipartimento di Chimica Strutturale e Stereochimica Inorganica e Centro CNR "CSSSCMTBSO"
Università di Milano, via Venezian 21
20133 Milano (Italy)
E-mail: norberto.masciocchi@uninsubria.it

[c] Prof. N. Masciocchi
Dipartimento di Scienze Chimiche, Fisiche e Matematiche
Università dell'Insubria, via Valleggio 11
22100 Como (Italy)
Fax: (+39) 031 238 6119

  0947-6539/02/0808-1813 $ 20.00+.50/0

ethanol solutions of the corresponding potassium soaps with a stoichiometric amount of cobalt(II) acetate tetrahydrate, according to the classical precipitation method generally used in the synthesis of heavy metal soaps [Eqs. (1) – (4)].[4, 5]

$$CH_3(CH_2)_{n-2}COOH + KOH \rightarrow CH_3(CH_2)_{n-2}COOK + H_2O \quad (1)$$

$$HOOC(CH_2)_{n-2}COOH + 2\,KOH \rightarrow KOOC(CH_2)_{n-2}COOK + 2\,H_2O \quad (2)$$

$$2\,CH_3(CH_2)_{n-2}COOK + [Co(CH_3COO)_2 \cdot 4H_2O] \rightarrow [Co\{CH_3(CH_2)_{n-2}COO\}_2(H_2O)_2] + 2\,H_2O + 2\,CH_3COOK \quad (3)$$

$$KOOC(CH_2)_{n-2}COOK + [Co(CH_3COO)_2 \cdot 4H_2O] \rightarrow [Co\{OOC(CH_2)_{n-2}COO\}(H_2O)_2] + 2\,H_2O + 2\,CH_3COOK \quad (4)$$

Carried out under mild experimental conditions (low temperature and high dilution), this precipitation method was thought to be well adapted for easy control of the degree of solvation and oxidation of the metal atoms without the lengthy purifications and recrystallisations necessary in the fusion method; obviously, only anhydrous species are likely to be formed by the latter technique. To ensure their chemical (and magnetic) purity, and the coordination geometry and oxidation state of the metal atoms, special care was taken to choose the most efficient operating conditions (nature and purity of reactants and solvents, concentration and temperature, stoichiometry, etc.).

Obtained as pink powders,[6] the compounds synthesised by this procedure were examined by scanning electron microscopy (SEM); they were typically found to consist of well-defined diamond-shaped platelets a few μm wide and less than 0.5 μm thick (Figure 1).

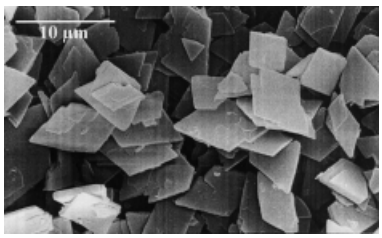

Figure 1. Characteristic view of the morphology of the powders of ***m*-*n*Co** and ***d*-*n*Co** compound as observed by scanning electron microscopy.

Their chemical formula (specifically the presence of exactly two carboxylate groups and two water molecules per cobalt atom) was ascertained by a set of complementary analytical techniques (elemental analysis, oxidising pyrolysis, mass spectroscopy, thermogravimetry and Karl Fischer titration), demonstrating the consistency of the whole series of samples (Table 1). In addition, preliminary information on the structural features of these species was supplied by FT-IR and UV/Vis/NIR spectroscopy, which suggested the presence of hydrogen-bonded water molecules, of bidentate carboxylate groups and of cobalt(II) atoms of nearly octahedral coordination geometry (see below). These analytical results were fully confirmed by our XRPD studies discussed below.

Crystal structure: The crystal structure of the compounds was investigated by XRPD methods. The RT XRPD patterns recorded contain up to eight equidistant sharp reflections

Table 1. Number of carboxylate groups[a] and water molecules[b] per cobalt atom in compounds ***m*-*n*Co** and ***d*-*n*Co**.

Compounds	COO	H_2O^{KF}	H_2O^{OP}	H_2O^{EA}
***m*-12Co**	2.02	1.9	2.0	1.9
***m*-14Co**	1.96	1.8	1.6	2.0
***m*-16Co**	1.99	1.8	1.8	1.9
***m*-18Co**	1.98	2.2	1.8	1.9
***m*-20Co**	1.99	1.8	1.7	1.9
***m*-22Co**	1.98	2.0	1.5	1.9
***d*-8Co**	1.98	1.9	1.9	2.1
***d*-10Co**	2.00	1.7	1.9	1.8
***d*-12Co**	1.97	2.3	1.9	2.1
***d*-14Co**	1.97	2.4	1.9	2.2
***d*-16Co**	1.96	2.2	1.8	2.2

[a] The number x was deduced from carbon and cobalt contents (determined by elemental analysis and oxidising pyrolysis, respectively) by means of chemical formulas $[Co\{CH_3(CH_2)_{n-2}COO\}_x(H_2O)_y]$ and $[Co\{OOC(CH_2)_{n-2}COO\}_{x/2}(H_2O)_y]$. [b] The number y was deduced from water contents measured by Karl Fisher titration (KF), cobalt content measured by oxidising pyrolysis (OP), and carbon content measured by elemental analysis (EA), by means of the above chemical formulas with $x = 2$.

(00*l*) in the low-angle region, indicative of a lamellar structure similar to that generally observed with metal soaps.[7–9] As later confirmed by the complete solution and refinement of the crystal structures of selected samples (***d*-12Co**,[1] ***m*-12Co** and ***m*-20Co**), the polar head groups of the molecules are segregated from the alkyl chains to form well-defined polar sublayers; the alkyl chains are fully extended in a planar zigzag conformation and arranged in single or double layers with a slight tilt with respect to the layer normal. The stacking period of the layers, deduced from the low-angle Bragg reflections (Figure 2), increases linearly with the chain length (n) according to the Equations (i) and (ii) below, each one characterising one homologous series.

$$\textbf{\textit{m}-\textit{n}Co} \qquad d\,[\text{Å}] = (6.48 \pm 0.50) + (2.52 \pm 0.03)\,n \quad (i)$$

$$\textbf{\textit{d}-\textit{n}Co} \qquad d\,[\text{Å}] = (4.57 \pm 0.28) + (1.26 \pm 0.02)\,n \quad (ii)$$

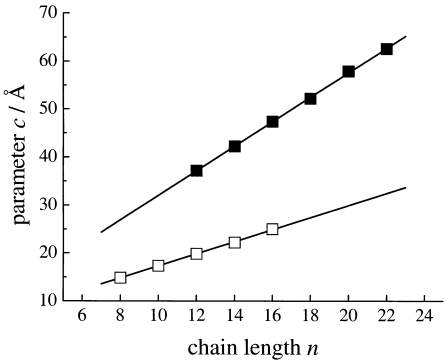

Figure 2. Variation of the stacking period in the crystalline ***m*-*n*Co** (■) and ***d*-*n*Co** (□) series as a function of the number of carbon atoms within the alkanoate moieties.

The slopes of the $d(n)$ straight lines (2.52 Å/carbon atom for ***m*-*n*Co** and 1.26 Å/carbon atom for ***d*-*n*Co**), when compared to the slope found for the orthorhombic crystals of linear

0947-6539/02/0808-1814 $ 20.00+.50/0 *Chem. Eur. J.* **2002**, *8*, No. 8

paraffins (1.27 ± 0.01 Å),[10] indicate that the alkyl chains, standing upright in the layers, are most likely arranged in double layers in the ***m-n*Co** and single layers in the ***d-n*Co** series of compounds.

In addition, the XRPD patterns contain a great number of extra sharp reflections in the wide-angle region, a feature that is only rarely reported in the literature on soaps; this indicates a well-developed three-dimensional crystalline arrangement. The *d* values associated with these reflections generally depend on the chain length, except for some of them whose spacing remains constant and which correspond to the in-layer packing mode of the molecules. Too intricate to be interpreted straight away in terms of three-dimensional crystal lattices using conventional cell determination procedures, the patterns were indexed thanks to additional information provided by selected-area electron diffraction (SAED) experiments.

As mentioned above, SEM observations showed that the powder samples consist of well-defined platelike crystallites, thus enabling SAED experiments on isolated platelets oriented perpendicularly to the electron beam. The ED patterns of all species are identical. One such pattern is shown in Figure 3. They contain an extended set of sharp reflections ((*hk0*), all present in the XRPD trace), consistent with a *primitive* rectangular two-dimensional lattice of cell parameters $a \approx 9.6$ Å and $b \approx 7.5$ Å. The absence of arched or split reflections and of parasitic scattering indicates clearly the single-crystalline texture of the platelets and the good quality of their crystal ordering. It is important to note that reflections indexed as (400), (210), (020), (420), (230), (040), and so on (i.e., those with $h/2+k=2n$), the spacing of which is nearly independent of the chain length, are distinctly more intense than the others (as expected from the upright orientation of the alkyl chains in the platelets; see below). Interestingly enough, the derived *centred* rectangular sublattice ($a' = a/2 \approx 4.8$ Å, $b' = b \approx 7.5$ Å) built upon these reflections (Figure 3) is identical to the two-dimensional crystal lattice that describes the lateral packing of linear paraffins in the orthorhombic form,[11] and suggests a similar packing for the alkyl chains in the soap crystals.

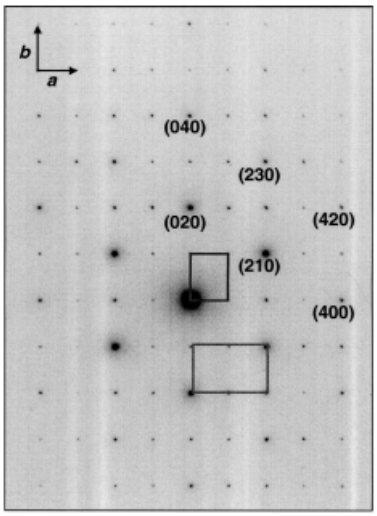

Figure 3. Characteristic electron diffraction pattern recorded with the platelets oriented perpendicularly to the electron beam. The rectangles correspond to the (a^*,b^*) cell of the present compounds (small) and of the paraffin-like subcell (large).

Using the information from SAED, along with the knowledge of the lamellar period determined from the small-angle reflections, we indexed the XRPD patterns of the present compounds (using U-FIT[12] for standard least-squares refinements and FULLPROF[13] for full pattern matching) with monoclinic lattices of cell parameters[14] (Figures 4 and 5).

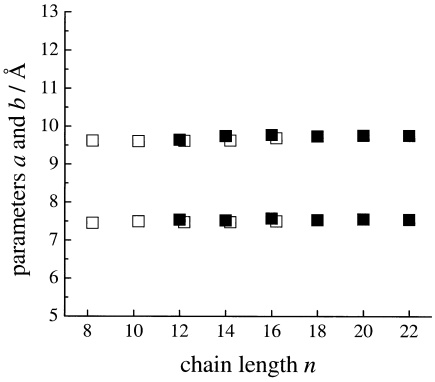

Figure 4. Crystal parameters *a* and *b* of the monoclinic cells refined for ***m-n*Co** (■) and ***d-n*Co** (□) compounds. For the sake of clarity, the points corresponding to the ***d-n*Co** series are slightly shifted to the right.

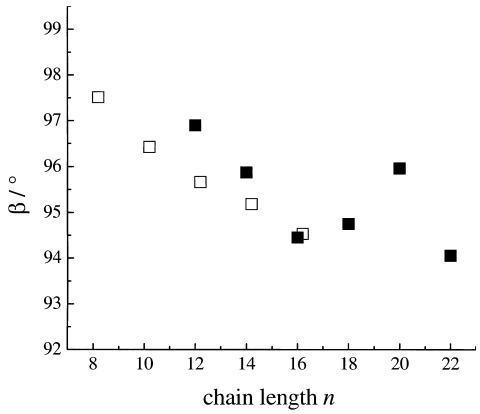

Figure 5. Monoclinic angle β of the cells refined for ***m-n*Co** (■) and ***d-n*Co** (□) compounds. For the sake of clarity, the points corresponding to the ***d-n*Co** series are slightly shifted to the right.

For ***m-n*Co**, the results were:

$a = 9.59 \pm 0.01$ Å
$b = 7.53 \pm 0.01$ Å
$c = d/\sin\beta = (6.44 \pm 0.45) + (2.56 \pm 0.03) \times n$ Å
$\beta = 95.3 \pm 0.1^\circ$

For ***d-n*Co**, they were:

$a = 9.63 \pm 0.01$ Å
$b = 7.41 \pm 0.01$ Å
$c = d/\sin\beta = (4.74 \pm 0.21) + (1.26 \pm 0.02) \times n$ Å
$\beta = 95.9 \pm 0.1^\circ$

The detailed crystal structures of ***m*-12Co** and ***m*-20Co** were established by ab initio XRPD techniques and successfully refined by the Rietveld method (see Experimental Section). As shown in Figure 6, both structures contain rather elongated cells, which are consistent with the long aliphatic

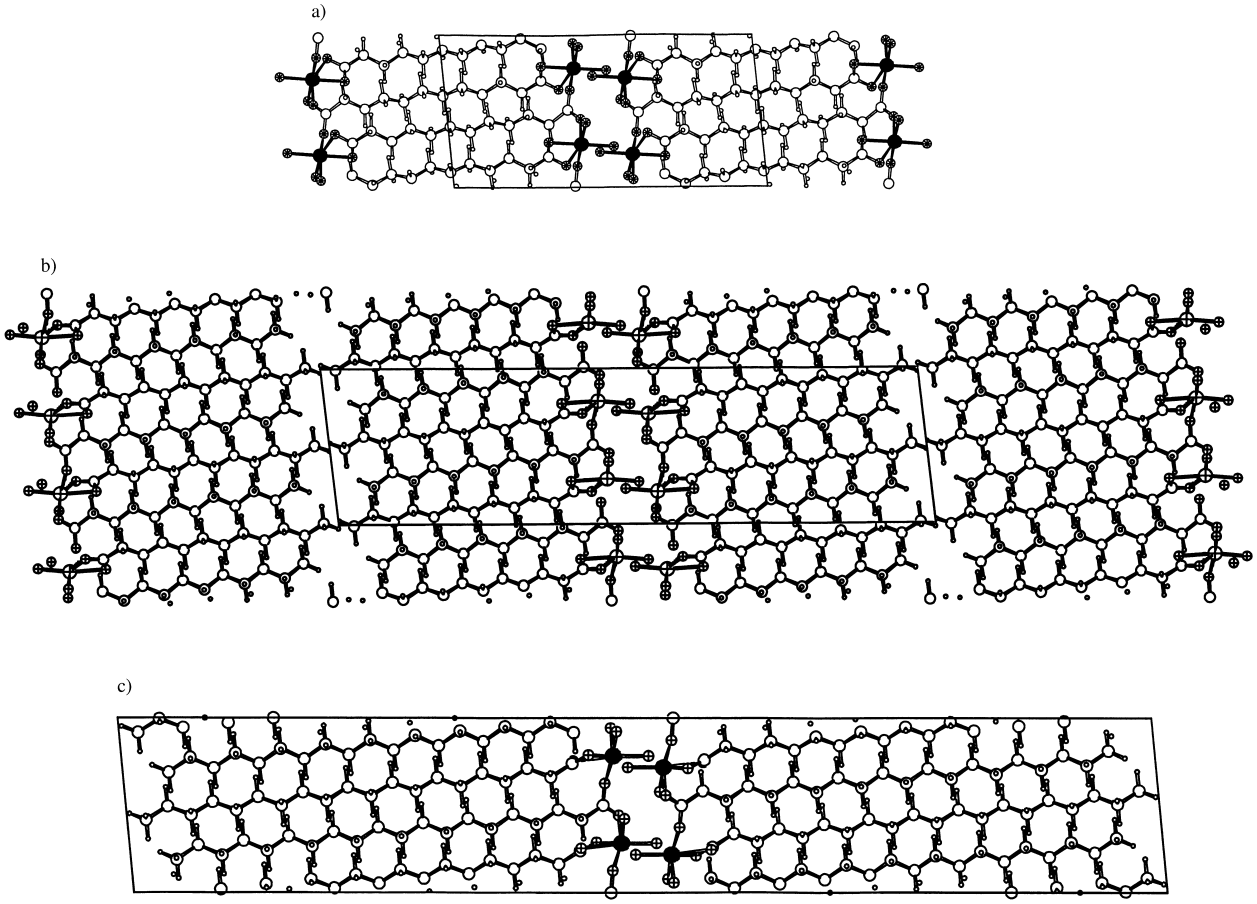

Figure 6. Schematic plot (viewed down *b*, horizontal axis = *c*) of the unit cell for a) ***d*-12Co**, b) ***m*-12Co** and c) **m-20Co**, showing the elongated organic ligands running nearly parallel to the *c* axes; cobalt atoms in black, oxygen atoms crossed. In order to highlight the bilayer structure of the ***m*-*n*Co** series, a larger portion of the crystal structure of ***m*-12Co** is shown.

chains in the all-*trans* mode. The two species are strictly isomorphous, belonging to the $P2_1/a$ space group, and manifest the same structural features.

Pseudooctahedral cobalt(II) atoms are bonded to two *cis* water molecules, as well as to two chemically, and crystallographically, unequivalent alkanoates. One carboxylato group is chelating [η^2-O,O] and the other bridges, in the [μ-O,O] mode, two cobalt ions which are about 6.3 Å apart in ***m*-12Co** and ***m*-20Co**, and about 5.90 Å apart in ***d*-12Co**. The bridging RCO_2 fragments, which have an *anti*–*anti* conformation (see Scheme 1), form (-OCO-Co-)$_n$ chains zigzagging along the *a* direction. Consistent with the glide symmetry operation, the chiral configuration of each cobalt atom alternates along the chains.

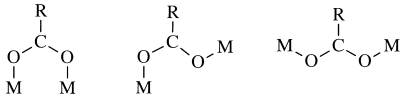

syn - syn *syn - anti* *anti - anti*

Scheme 1. The three conformations for metal–carboxylate–metal bridges.

The fully stretched alkanoate groups are arranged in slabs (with polar heads and hydrophobic tails), slightly tilted with respect to *c* and standing virtually perpendicular to the (*a*,*b*) plane, are nearly parallel, and show a mutual match between the lipophilic sections of the slabs. This double-layer arrangement is also typical for purely organic long-chain alkanoates and related polymeric soaps (acid sodium palmitate and lead azelate[15]). Thus, we may safely state that, no matter what the end group is, for such a versatile class of compounds segregation of the lipophilic tails (adoption of a fully stretched conformation) invariably occurs, with the polar heads typically facing each other about inversion centres.[16] Consistently, the crystal structure of ***d*-12Co**, in which each dicarboxylate binds two different cobalt ions in the two above-mentioned modes, has similar features (apart from the obvious apolar nature of each *centrosymmetric* slab with a halved *c* axis—see Figure 6), and crystallises in $P2_1/a$ with nearly equivalent metal coordination geometry and overall packing features of the organic ligands.

As will be mentioned below, a significant anisotropic broadening of the XRPD reflections was observed, the narrowest peaks belonging to the 00*l* class. Since the shape of the crystals observed by electron microscopy and the actual lamellar structure derived from XRPD data do not favour an interpretation based on the limited thickness of the crystallites in the *a* and *b* directions (see Figure 1), we propose that a slight rotational (i.e., azimuthal) disorder about the long axis might be present in the alkyl tails, thus affecting only reflections with h or $k \neq 0$. Indeed, a very recent single-crystal

  0947-6539/02/0808-1816 $ 20.00+.50/0 *Chem. Eur. J.* **2002**, *8*, No. 8

analysis on hemiaquated manganese alkanoates has shown that, when the length of the alkyl residues is increased, such rotational disorder disrupts the quality of the crystals, preventing the meaningful modelling of the diffraction data of the highest terms.[17]

Spectroscopic properties: As already discussed for ***d*-12 Co** in a previous paper,[1] the IR and UV data collected for all the present compounds (see Experimental Section) are consistent with their crystal structure. The IR spectra exhibit clear bands characteristic of the different vibration modes of the C–H bonds for alkyl chains in a fully stretched all-*trans* conformation. As for the carboxylate groups, the frequency difference between the symmetric and antisymmetric C–O vibrations, $\Delta\tilde{\nu} = 128\ cm^{-1}$, is smaller than that observed for the corresponding ionic potassium soap ($\Delta\tilde{\nu}_i \approx 150\ cm^{-1}$) as required by the bidentate coordination mode of the carboxylic groups; because of the band widths, it is not possible to distinguish the chelating mode from the bridging mode both present in the structure.[18] The presence of two broad $\tilde{\nu}$O–H bands in the range $3200-3400\ cm^{-1}$ is related to the two aqua ligands implicated in hydrogen bonds, whose presence is also suggested by distances between oxygen atoms deduced from the structure analysis, thus bearing out the role these bonds play in the cohesion of the polar layers. The absorption band observed at $1670\ cm^{-1}$ is typical of compounds in which water molecules are strongly bonded to the metal centres. Finally, the UV spectra corroborate the pseudooctahedral geometry of Co^{II} ions.[19, 20] The values of Dq ($\sim 950\ cm^{-1}$) and Racah's parameter B ($\sim 846\ cm^{-1}$), estimated from the observed absorption bands, indicate a low crystal field ($Dq/B \approx 1.1$) in favour of the high-spin configuration observed for the metal centres (see below).

Magnetic properties: The magnetic properties of the present series of compounds were investigated, and great similarities were found between the carboxylate and the dicarboxylate series. This is illustrated here by the data corresponding to ***m*-20 Co** and ***d*-12 Co**, which are representative of their series. The susceptibility χ (suitably corrected for sample and holder diamagnetism) grows smoothly with decreasing temperature (Figures 7 and 8), following the Curie–Weiss law $\chi = C/(T-\theta)$ at temperatures higher than 200 K.

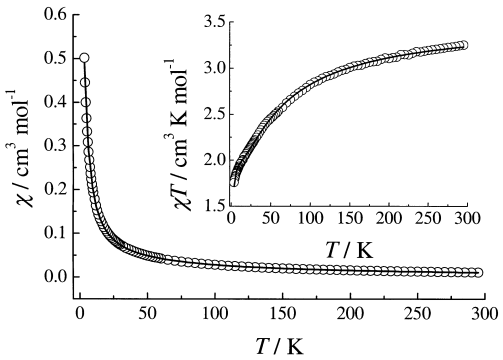

Figure 7. Temperature variation of the magnetic susceptibility χ of compound ***m*-20 Co**. Inset: χT vs. T variation. The unbroken lines correspond to the best fit of the experimental data with the relation given in the text.

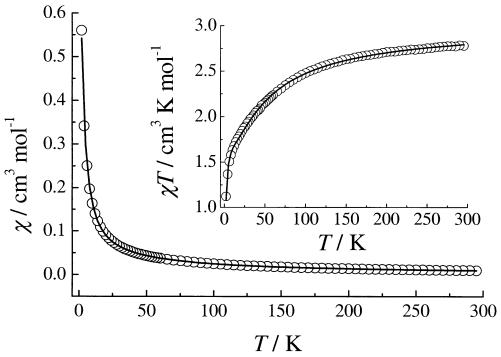

Figure 8. Temperature variation of the magnetic susceptibility χ of compound ***d*-12 Co**. Inset: χT versus T variation. The unbroken lines correspond to the best fit of the experimental data with the relation given in the text.

The values of the Curie constant reported in Table 2 are consistent with that expected for six-coordinated high-spin Co^{II} ions ($C \approx 2.8-3.4\ cm^3\,K\,mol^{-1}$).[21] The values of the Weiss temperatures θ are very similar for all the compounds and exhibit no systematic variation with the length of the carbon chain or the nature (i.e., mono- or dicarboxylate) of the organic ligand. The variation of the product χT as a function of temperature shows a continuous decrease with T between 295 K ($3.2\ cm^3\,K\,mol^{-1}$ for ***m*-20 Co** and $2.76\ cm^3\,K\,mol^{-1}$ for ***d*-12 Co**) and 2 K (1.75 and $1.08\ cm^3\,K\,mol^{-1}$, respectively) in agreement with the negative sign of the Weiss temperatures. These features may be explained by the existence of antiferromagnetic exchange interactions and the effect of spin–orbit coupling, known to exist for Co^{II} ions,[21–23] which most certainly contributes to the decay of χT upon cooling; the latter, however, does not explain entirely the decay observed, especially for the ***d*-n Co** series. Indeed, the temperature dependence of the effective magnetic moment deduced from the experimental data differs from that calculated for isolated Co^{II} ions.[1] In particular, the χT value measured at 2 K ($1.08\ cm^3\,K\,mol^{-1}$) is significantly smaller than expected ($1.8\ cm^3\,K\,mol^{-1}$) for isolated Co^{II} magnetic

Table 2. Curie constants, Weiss temperatures, and energies related to spin–orbit coupling effect (E_1)[a] and in-chain magnetic exchange interaction (E_2)[a] for compounds ***m*-n Co** and ***d*-n Co**.[b]

Compounds	C [$cm^3\,K\,mol^{-1}$]	Θ [K]	$-E_1/k$ [K]	$-E_2/k$ [K]
***m*-12 Co**	3.5	−17.4	−52.9	−0.72
***m*-14 Co**	3.7	−34.9	−65.0	−0.71
***m*-16 Co**	3.7	−33.2	−61.6	−0.66
***m*-18 Co**	3.6	−24.8	−56.5	−0.58
***m*-20 Co**	3.5	−31.8	−64.2	−0.69
***m*-22 Co**	3.3	−28.8	−61.1	−0.52
***d*-8 Co**	3.1	−10.9	−52.0	−1.24
***d*-10 Co**	3.0	−20.3	−58.4	−0.87
***d*-12 Co**	3.0	−19.7	−56.6	−1.03
***d*-14 Co**	3.1	−22.0	−56.4	−1.01
***d*-16 Co**	3.0	−28.3	−58.8	−0.97

[a] The energies E_1 and E_2 were determined by the two exponential functions described in the text. [b] Typical errors are in the 1–5% range.

centres. In addition, the magnetisation curve $M(H)$ shown in Figure 9, saturating at $M_S = 2.2\,\mu_B\,mol^{-1}$ as expected ($2-3\mu_B\,mol^{-1}$),[21, 22] is significantly lower than that predicted by Brillouin's law,[21] $M(H) = NgJ\mu_B B_J(\eta)$, where J is the total

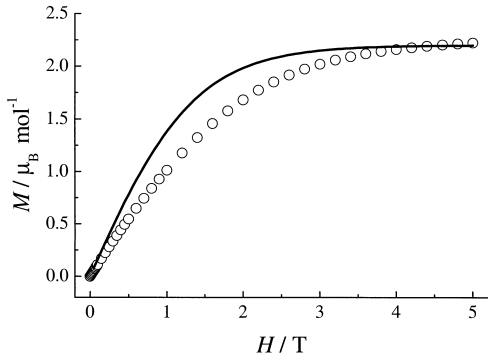

Figure 9. Magnetisation vs. field curve at 2 K for compound ***d*-12Co**. The unbroken line corresponds to Brillouin's law scaled to the saturation value.

angular momentum, $\eta = g\mu_B H/kT$, and $B_J(\eta) = 1/J[(J+½)\coth(J+½)\eta - ½\coth(\eta/2)]$. This situation seems less apparent for the other series, ***m*-*n*Co**, where its behaviour is closer to that expected for quasi-isolated cobalt(II) ions. In particular the magnetisation versus field curve shown in Figure 10 is relatively well fitted by the Brillouin function, pointing to weaker antiferromagnetic exchange compared to the **d-*n*Co** series.

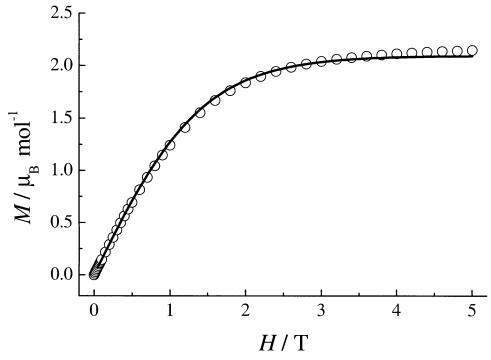

Figure 10. Magnetisation vs. field curve at 2 K for compound ***m*-20Co**. The unbroken line corresponds to the best fit to Brillouin's law.

Looking at the structure, the weak antiferromagnetic coupling suggested by the experimental data very likely goes through the carboxylato bridges along the $(\text{-OCO-Co-})_n$ chains, the exchange pathway through the hydrogen bonds appearing less effective, even if shorter.[24] No analytical expression is available in the literature describing the temperature dependence of χT for chains of Co^{II} ions with spin–orbit coupling. In addition, the low-temperature approximation, which consists in treating the Co^{II} ions as anisotropic pseudospins $S = ½$ below 30 K,[21, 23] leading thus to an Ising-like chain system, is not satisfactory in the present series of compounds mainly because the exchange interaction is too weak to show up clearly against the spin–orbit coupling. In order to get an estimate of the strength of the antiferromagnetic exchange interaction, it has been shown in previous work[1] that one may use the simple phenomenological Equation (iii),[25] where $A+B$ equals the Curie constant, and E_1, E_2 hold for "activation energies" corresponding to the spin–orbit coupling and to the antiferromagnetic exchange

$$\chi T = A\exp(-E_1/kT) + B\exp(-E_2/kT) \qquad \text{(iii)}$$

interaction, respectively. This Equation describes the spin–orbit coupling well; this coupling results in a splitting between discrete levels, and exponential low-temperature divergence of the susceptibility ($\chi T \propto \exp(\alpha J/2kT)$). All the experimental data of the present work have been fitted (by a least-squares refinement method) and are very well described by this model (Figures 7 and 8). The results are summarised in Table 2. The values found for $C = A+B$ agree with those obtained from the Curie–Weiss law in the high temperature range (see above), and the values for E_1/k are consistent with those given in the literature for both the effects of spin–orbit coupling and site distortion (E_1/k of the order of 100 K).[21] As for the value found for the antiferromagnetic exchange interaction, it is very weak indeed, with mean values $-E_2/k = -0.65$ K and $-E_2/k = -1.02$ K for ***m*-*n*Co** and ***d*-*n*Co**, respectively, corresponding to interactions $J = -1.30$ and -2.04 K within the Ising chain approximation ($\chi T \propto \exp(+J/2kT)$).[21, 23] As expected from the experimental behaviours discussed above, the exchange coupling is weakest for the ***m*-*n*Co** series. The shorter distance between neighbouring cobalt(II) atoms observed in the ***d*-12Co** species, and presumably in the whole ***d*-*n*Co** series, can be assumed to be responsible for the slightly larger antiferromagnetic exchange interaction values measured for the ***d*-** than for the ***m***-series.

Conclusion

The cobalt compounds investigated in the present work comprise a new family of carboxylate-bridged chain complexes of Co^{II}: the ***m*-*n*Co** and ***d*-*n*Co** series are homologous series that form layered compounds, which have been fully characterised both magnetically and structurally. The rare[26] *anti–anti* conformation mode of the μ-RCOO groups, recently proposed for ***d*-12Co**, is here confirmed for two selected examples of the ***m*-*n*Co** series, thanks to XRPD, which, for the first time, allowed the determination of the complete three-dimensional structure of transition metal soaps containing long-chain alkanoates. The XRPD method used combined the power of the ab initio technique (particularly the simulated annealing procedure, which allowed formulation of the correct structural model) with that of selected-area electron diffraction. Interestingly, some of the structural features reported above were correctly predicted in old reports, when only a few d spacings, mostly attributed to basal reflections, were known;[5, 7] however, the quantitative assessment of the lattice parameters and symmetry, together with details on the overall packing and connectivity (i.e., the structure) were, until now, out of reach; the complete characterisation of these rather complex phases demonstrates, again, that, in the absence of suitable single crystals, restrained XRPD refinements, although lacking atomic reso-

0947-6539/02/0808-1818 $ 20.00+.50/0 *Chem. Eur. J.* **2002**, *8*, No. 8

lution, may provide significant and otherwise inaccessible information to the structural chemist.

Furthermore, the magnetic properties of all the compounds have been analysed in detail and interpreted on the basis of their crystal structures. Only a few examples have been reported for one-dimensinal transition metal polymers where the exchange effectively goes through carboxylato bridges of various geometries (see Scheme 1);[27] for example, extensive work on Cu^{II} complexes has shown that the exchange coupling is strongly antiferromagnetic with a *syn–syn* conformation,[28] very weakly so (possibly ferromagnetic[29]) with a *syn–anti* conformation,[30] and weak-to-medium antiferromagnetic with an *anti–anti* conformation.[31] The results presented above confirm that the *anti–anti* geometry of the diaquacobalt(II)dicarboxylate favours very weak antiferromagnetic interactions and also that the mono- or dicarboxylic nature of the alkanoates may have an effect on the magnitude of the exchange coupling in relation to small structural variations. Further work can be anticipated in preparing and characterising anhydrous, or differently solvated, analogues.

Experimental Section

General remarks: Thermogravimetric experiments were performed on a Setaram TG 92 instrument (heating rate of 2 °C min^{-1}, air stream). Mass spectroscopy experiments were carried out by means of a Micro Mass Trio 2000 instrument (degassing of quartz crucible at 100 °C, desolvation of soap at 200 °C). Scanning electron microscopy observations were made with a JEOL JSM-840 instrument. Electron diffraction experiments were performed with a transmission Philips CM 12 instrument equipped with a PW 6594 goniometer (120 kV). FT-IR studies used an ATI Mattson Genesis computer-driven instrument (0.1-mm thick powder samples in KBr). UV/Vis/NIR studies were performed on a Perkin–Elmer Lambda 19 instrument (spectra recorded by reflection with a resolution of 4 nm and a sampling rate of 480 nm min^{-1}). Magnetic studies were carried out by means of a Quantum Design XMPMS SQUID magnetometer. Susceptibilities were measured at 0.2 T in the temperature range 1.7–295 K. The magnetisation curve was determined at 2 K with an applied field ranging from 0 to 5 T.

In the X-ray powder diffraction experiments, the samples were cautiously deposited in the hollow of a side-loaded holder. The data were collected on a Siemens D 500 diffractometer equipped with Soller slits, a primary-beam curved quartz monochromator ($Co_{K\alpha 1}$, $\lambda = 1.78897$ Å), a Na(Tl)I scintillation detector and a pulse height amplifier discriminator. The generator was operated at 35 kV and 30 mA. Slits used: divergence 1.0°, antiscatter 1.0° and receiving 0.15 mm. Long overnight scans were performed in the range $2 < 2\theta < 130°$, with θ:2θ step-scanning mode [$\Delta 2\theta = 0.02°$ and $t = 10$ s]. The indexing procedure is described in the text.

Potassium *n*-alkanoate, $C_nH_{2n-1}KO_2$ ($12 \le n \le 22$) and potassium *n*-alkane-α,ω-dioate, $C_nH_{2n-2}K_2O_4$ ($8 \le n \le 16$): An aqueous solution of KOH (Titrisol 0.1N, Fluka) (0.1 mol) diluted with acetone (Carlo Erba, analysis) (150 mL) was added dropwise to a stirred solution of *n*-alkanoic (0.1 mol) and *n*-alkane-α,ω-dioic (0.05 mol) acid (Lancaster, 99%) in acetone (500 mL), and the mixture was heated under reflux for 3 h (56.5 °C). After cooling to room temperature, the white precipitate of potassium soap formed was filtered, repeatedly washed with hot acetone and dried in vacuum at room temperature for 12 h (yield >90%).

Diaquacobalt(II) *n*-alkanoate, $[Co\{CH_3(CH_2)_{n-2}COO\}_2(H_2O)_2]$ ($12 \le n \le 22$), *m*-*n*Co, and diaquacobalt(II) *n*-alkane-α,ω-dioate, $[Co\{OOC(CH_2)_{n-2}COO\}(H_2O)_2]$ ($8 \le n \le 16$), *d*-*n*Co: Potassium soap (1.96 g) was dissolved in a mixture of demineralised water (18.2 MΩ cm, Millipore) and ethanol (Carlo Erba, purum) (300 mL, 1:1 *v*/*v*) and added dropwise to a stirred solution of $[(CH_3COO)_2Co \cdot 4H_2O]$ (Aldrich, 99.999%) (stoichiometric amount) in demineralised water (40 mL) at 20 °C. After the mixture had been stirred for 3 h, the pink precipitate of the corresponding diaquacobalt soap was filtered, repeatedly washed with aqueous ethanol (1:1 *v*/*v*) and dried under vacuum at room temperature for 24 h (yield 70–95%). The presence of water molecules was detected by thermogravimetry (TGA) [weight losses (%) at about 90 °C: 6.4 for ***m*-12Co**, 5.6 for ***m*-14Co**, 5.4 for ***m*-16Co**, 5.1 for ***m*-18Co**, 4.8 for ***m*-20Co**, 4.3 for ***m*-22Co**, 13.1 for ***d*-8Co**, 12.0 for ***d*-10Co**, 10.8 for ***d*-12Co**, 9.2 for ***d*-14Co**, 8.0 for ***d*-16Co**] and ascertained by mass spectrometry. Purity was confirmed by elemental analysis (EA) [calcd (%) for ***m*-12Co** (493.3): C 58.4, H 10.2; found C 58.6, H 10.2; calcd (%) for ***m*-14Co** (547.3): C 61.2, H 10.6; found C 61.1, H 10.7; calcd (%) for ***m*-16Co** (603.4): C 63.4, H 11.0; found C 63.7, H 11.1; calcd (%) for ***m*-18Co** (559.5): C 65.3, H 11.3; found C 65.4, H 11.4; calcd (%) for ***m*-20Co** (715.5): C 66.9, H 11.5; found C 67.1, H 11.6; calcd (%) for ***m*-22Co** (771.6): C 68.3, H 11.7; found C 68.4, H 11.8; calcd (%) for ***d*-8Co** (267.0): C 36.0, H 6.0; found C 35.8, H 6.0; calcd (%) for ***d*-10Co** (295.0): C 40.7, H 6.8; found C 41.1, H 6.9; calcd (%) for ***d*-12Co** (323.0): C 44.6, H 7.5; found C 44.3, H 7.5; calcd (%) for ***d*-14Co** (351.1): C 47.9, H 8.0; found C 47.5, H 8.0; calcd (%) for ***d*-16Co** (379.1): C 50.7, H 8.5; found C 50.1, H 8.5], oxidising pyrolysis (OP) [heating in air from 20 to 700 °C at 2 °C min^{-1}, 30 min stay at 700 °C to transform cobalt into Co_3O_4,[32, 33] and cooling to 20 °C at 10 °C min^{-1} (cobalt % given with an accuracy of 0.2%); ***m*-12Co**: calcd 11.9, found 11.9; ***m*-14Co**: calcd 10.7, found 10.9; ***m*-16Co**: calcd 9.7, found 9.8; ***m*-18Co**: calcd 8.9, found 9.1; ***m*-20Co**: calcd 8.2, found 8.3; ***m*-22Co**: calcd 7.6, found 7.7; ***d*-8Co**: calcd 22.1, found 22.2; ***d*-10Co**: calcd 20.0, found 20.1; ***d*-12Co**: calcd 18.2, found 18.4; ***d*-14Co**: calcd 16.8, found 16.9; ***d*-16Co**: calcd 15.5, found 15.8], and Karl Fischer (KF) titration of water (water % given with an accuracy of 0.3%) [***m*-12Co**: calcd 7.3, found 6.8; ***m*-14Co**: calcd 6.6, found 5.9; ***m*-16Co**: calcd 5.9, found 5.2; ***m*-18Co**: calcd 5.4, found 6.0; ***m*-20Co**: calcd 5.0, found 4.4; ***m*-22Co**: calcd 4.7, found 4.6; ***d*-8Co**: calcd 13.5, found 13.0; ***d*-10Co**: calcd 12.2, found 10.6; ***d*-12Co**: calcd 11.1, found 12.5; ***d*-14Co**: calcd 10.3, found 12.2; ***d*-16Co**: calcd 9.5, found 10.5]; IR (KBr pellet): $\tilde{\nu}$ (± 2 cm^{-1}) = 3401 (νOH–O), 3262 (νOH–O), 1670 ($\delta_b H_2O$), 2919 ($\nu_{as}CH_2$), 2850 ($\nu_s CH_2$), 1542 (ν_{as}C=O), 1470 ($\delta_s CH_2$), 1414 (ν_sC–O), 723 cm^{-1} (ρCH_2); UV/Vis (diffuse reflectance for octahedral coordination of Co^{II}): $\lambda = 1316$ ($^4T_{1g} \rightarrow {}^4T_{2g}$), 714 ($^4T_{1g} \rightarrow {}^4A_{2g}$), 543 nm ($^4T_{1g} \rightarrow {}^4T_{1g}(P)$).

Ab initio XRPD structure determination of *m*-12Co and *m*-20Co: Sample preparation, data collection and indexing procedures are described above. Systematic absences indicated $P2_1/a$ as the probable space group for both compounds, later confirmed by successful structure solution and refinement; density considerations suggested $Z = 4$. Given the rather complex structures of ***m*-12Co** and ***m*-20Co** (containing 31 and 47 crystallographically independent non-H atoms, respectively), neither EXPO[34] nor standard Patterson methods afforded unique, refinable cobalt atom locations that could later be used for model completion by Fourier methods. However, with the aid of the high-performance program TOPAS,[35] we successfully solved both structures by the simulated annealing technique[36] using two independent rigid all-*trans* alkanoate groups and one *cis*-$Co(H_2O)_2$ rigid fragment. Such models were later refined by introducing soft restraints into the Co–O distances, by freeing the R–CO_2 torsional angles, and by adding a proper description (in the fundamental parameters approach[37]) of the diffraction conditions. An overall isotropic thermal parameter was used, with data truncated, in the final stages of the refinements, in the 4–64° (2θ) range. Low-angle data suffer from beam overflow, sample misalignment, air scattering and extreme vertical divergence effects; the noisy data above 64° are mainly background, thus suggesting some structural disorder or high mobility of the swinging alkanoate tails (as discussed above). Minor systematic errors were corrected with the aid of sample-displacement angular shifts and preferred orientation corrections, with (001) pole. A second-order spherical harmonics description of the reflection widths was found necessary in order to account for anisotropic broadening effects, which are particularly evident in the ***m*-20Co** species. Scattering factors, corrected for real and imaginary anomalous dispersion terms, were taken from the internal library of TOPAS. The final Rietveld refinement plots are shown in Figure 11.

Crystal data for *m*-12Co: $C_{24}H_{46}CoO_6$, formula weight 489.63 g mol^{-1}, monoclinic, $P2_1/a$; $a = 9.688(1)$, $b = 7.5495(9)$, $c = 37.281(5)$ Å, $\beta = 96.70(3)°$, $V = 2708.1(6)$ Å^3; $Z = 4$; $\rho = 1.198$ g cm^{-3}. Final R_p, R_{wp} and R_F agreement factors, for 3001 data points collected in the 4–64° range, are 0.139, 0.109 and 0.081, respectively.

Crystal data for *m*-20Co: $C_{40}H_{78}CoO_6$, formula weight 714.11 g mol^{-1}, monoclinic, $P2_1/a$; $a = 9.7260(7)$, $b = 7.5477(7)$, $c = 57.53(1)$ Å, $\beta =$

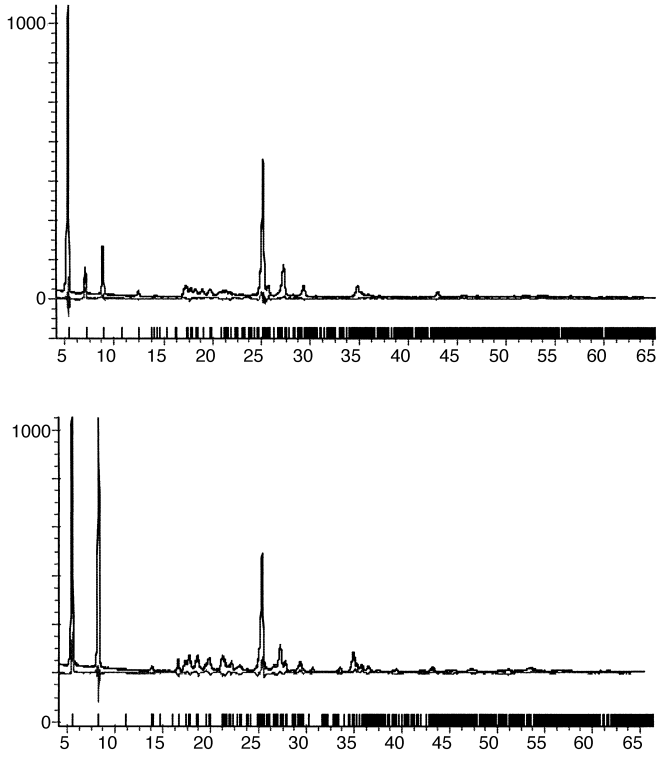

Figure 11. Rietveld refinement plot for compounds ***m*-12 Co** and ***m*-20 Co** in the 4–64° (2θ) range, with difference plot and peak markers at the bottom. The low-angle section, dominated by the strong (001) peak, has been omitted in order to highlight the agreement at intermediate angles. Horizontal axis: 2θ values [°]; vertical axis: intensity [a.u.].

94.66(4)°, $V = 4209.6(9)$ Å^3; $Z = 4$; $\rho = 1.122$ g cm^{-3}. Final R_p, R_{wp} and R_F agreement factors, for 3001 data points collected in the 4–64° range, are 0.115, 0.082 and 0.039, respectively.

CCDC-172131 and CCDC-172132 contain the supplementary crystallographic data for this paper. These data can be obtained free of charge via www.ccdc.cam.ac.uk/conts/retrieving.html (or from the Cambridge Crystallographic Data Centre, 12 Union Road, Cambridge CB21EZ, UK; (fax: (+44) 1223-336-033; or e-mail: deposit@ccdc.cam.ac.uk).

Acknowledgement

This is part of the PhD thesis work of one author (J.-M.R). We thank Prof. J. Guille, of the Institut de Physique et Chimie des Matériaux de Strasbourg, Strasbourg (France), for his contribution to the scanning electron microscopy, and Dr. M. Drillon for helpful discussions, Dr. B. Lotz from the Institut Charles Sadron, Strasbourg (France), for his contribution to the electron diffraction experiments, and Dr. A. Kern and Dr. A. Coelho (Bruker AXS) for providing the β version of the high-performance Topas-R program.

[1] J.-M. Rueff, N. Masciocchi, P. Rabu, A. Sironi, A. Skoulios, *Eur. J. Inorg. Chem.* **2001**, 2843.
[2] *Structure Determination from Powder Diffraction Data* (Ed.: B. David), *Newsletter No. 25*, Commission on Powder Diffraction, International Union of Crystallography, July **2001**.
[3] See, for example, a) K. N. Mehrotra, A. K. Kulshretrha, S. Verghese, *Tens. Surf. Det.* **1999**, *36*, 46; b) E. Rocca, G. Bertrand, C. Rapin, J.-C. Labrune, *J. Electroanal. Chem.* **2001**, *503*(*1–2*), 133; c) K. Binnemans, L. Jongen, C. Gorller-Walrand, W. D'Olieslager, D. Hinz, G. Meyer, *Eur. J. Inorg. Chem.* **2000**, 1429, and references therein.
[4] R. C. Mehrotra, R. Bohra, *Metal Carboxylates*, Academic Press, London, **1983**, p. 16.
[5] a) H. Kambe, *Bull. Chem. Soc. Jpn.* **1961**, *34*, 78; b) H. Kambe, *Bull. Chem. Soc. Jpn.* **1961**, *34*, 81.
[6] The preparation of blue or purple cobaltous soaps is reported in the literature, and mostly attributed to anhydrous or dehydrated specimens: H. Kambe, *Bull. Chem. Soc. Jpn.* **1961**, *34*, 1794, and references therein.
[7] a) R. D. Vold, G. S. Hattiangdi, *Ind. J. Chem.* **1949**, *41*, 2311; b) R. D. Vold, G. S. Hattiangdi, *Ind. J. Chem.* **1949**, *41*, 2320.
[8] A. Skoulios, *Ann. Phys.* **1978**, *3*, 421.
[9] K. Binnemans, L. Jongen, C. Bromant, D. Hinz, G. Meyer, *Inorg. Chem.* **2000**, *39*, 4938.
[10] A. I. Kitaigorodskii, *Organic Chemical Crystallography*, Consultants Bureau, New York, **1961**, p. 180.
[11] D. L. Dorset, *Structural Electron Crystallography*, Plenum Press, New York, **1995**.
[12] M. Evain, U-FIT: *A cell parameter refinement program*, I.M.N. Nantes (France), **1992**.
[13] J. Rodriguez-Carvajal, FULLPROF v. 3.2, Laboratoire Léon Brillouin, CEA CNRS, **1997**.
[14] Slight differences may appear with the values later quoted from the two full structure refinements on the *same* diffraction data, since a different, and more complex, approach has been used for correcting for instrumental parameters and optics.
[15] a) M. L. Lynch, F. Wireko, M. Tarek, M. Klein, *J. Phys. Chem.* **2001**, *105*, 552; b) F. Lacouture, M. François, C. Didjerjean, J. P. Rivera, E. Rocca, J. Steinmetz, *Acta Crystallogr. Sect. C* **2001**, *57*, 530.
[16] These polar slabs are also held together by hydrogen bonds between the water molecules and the carboxylic oxygens, which face each other at distances of about 2.70 Å. The separation between metal atoms of adjacent slabs (Co-O-H$\cdots$O-Co) is slightly less than 5 Å.
[17] Y. Kim, E. Lee, D.-Y. Jung, *Chem. Mater.* **2001**, *13*, 2684.
[18] K. Nakamoto, *Infrared and Raman Spectra of Organic and Coordination Compounds*, 4th ed., Wiley, New York, **1986**, p. 231.
[19] A. B. P. Lever, *Inorganic Electronic Spectroscopy*, 2nd ed., Elsevier, Amsterdam, **1984**.
[20] L. Banci, A. Bencini, C. Benelli, D. Gatteschi, C. Zanchini, *Struct. Bonding* **1982**, *52*, 37.
[21] R. L. Carlin, *Magnetochemistry*, Springer, Berlin, Heidelberg, **1986**.
[22] F. E. Mabbs, D. J. Machin, *Magnetism and Transition Metal Complexes*, Chapman & Hall, London, **1973**.
[23] O. Kahn, *Molecular Magnetism*, VCH, Weinheim, **1993**.
[24] B. N. Figgis, E. S. Kucharski, M. Vrtis, *J. Am. Chem. Soc.* **1993**, *115*, 176.
[25] P. Rabu, J.-M. Rueff, Z.-L. Huang, S. Angelov, J. Souletie, M. Drillon, *Polyhedron* **2001**, *20*, 1677.
[26] Occurring, among acyclic carboxylates, only in two polymeric derivatives: G. Liu, A. M. Arif, F. W. Bruenger, S. C. Miller, *Inorg. Chim. Acta* **1999**, *287*, 109.
[27] E. Colacio, J. M. Dominguez-Vera, J. P. Costes, R. Kivekäs, J. P. Laurent, J. Ruiz, M. Sundberg, *Inorg. Chem.* **1992**, *31*, 774.
[28] B. N. Figgis, R. L. Martin, *J. Chem. Soc.* **1956**, 3837.
[29] D. K. Toxle, S. K. Hoffmann, W. E. Hatfield, P. Singh, P. Chanduri, *Inorg. Chem.* **1988**, *27*, 394.
[30] R. L. Carlin, K. Kopinga, O. Kahn, M. Verdaguer, *Inorg. Chem.* **1986**, *25*, 1786.
[31] M. Kato, Y. Muto, *Coord. Chem. Rev.* **1988**, *92*, 45.
[32] J. Amiel, J. Besson, *Nouveau Traité de Chimie Minérale*, *Vol. 17* (Ed.: P. Pascal), Masson (Paris), **1963**.
[33] M. A. Mohamed, S. A. Halawy, M. M. Ebrahim, *J. Thermal Anal.* **1994**, *41*, 387–404.
[34] A. Altomare, M. C. Burla, G. Cascarano, G. Giacovazzo, A. Guagliardi, A. G. G. Moliterni, G. Polidori, *J. Appl. Crystallogr.* **1995**, *28*, 842.
[35] A. Kern, A. Coelho, TOPAS-R, Bruker AXS GmbH, Karlsruhe (Germany), **2001**.
[36] A. A. Coelho, *J. Appl. Crystallogr.* **2000**, *33*, 899.
[37] R. W. Cheary, A. A. Coelho, *J. Appl. Crystallogr.* **1998**, *31*, 862, and references therein.

Received: November 12, 2001 [F3678]

  0947-6539/02/0808-1820 $ 20.00+.50/0